

ZEOLITE FORMATION USING STRUCTURAL DIRECTING AGENT TO ENHANCE HEAVY NAPHTHA VIA REFORMING PROCESSES

Raghed Y. Ghazal, *Ahmed G. S Al-Azzawi, Mohammed H. Ali

Chemistry department, College of Education for Pure Science, University of Mosul, Iraq. *e-mail: amsss82@uomosul.edu.iq

Received 13.06.2024 Accepted 24.08.2024

Abstract: H-Zeolite was successfully prepared from a homogenous solution under controlled conditions using a thermal approach with tetramethylammonium bromide as an organic structural directing agent (OSDA), which adjusts the pores size of zeolitic networks and then increases the catalyst efficiency. The synthesized H-zeolite particles were characterized by X-ray Diffraction (XRD) analysis, X-ray Fluorescence (XRF) analysis, Scanning Electron Microscopy (SEM) analysis, Brunauer Emmett and Teller (BET) in order to ascertain the formation of pure crystalline phase and chemical structure. The zeoliting reactions of heavy naphtha were performed using the Teflon-lined autoclaves at 300 °C for 1, 2, and 3 hours separately. The gasoline reformate yields were evaluated by different techniques including RON, ¹H NMR, FTIR, and PIONA (GC-Mass) to investigate their characters and chemical contents. It was found that the loading of 2% of zeolite during the reforming reaction of heavy naphtha for 3 hours exhibited high conversion with high aromatic content, which resulted in a high RON (85) gasoline reformate. This study aims to employ a new approach to enhance Iraqi heavy naphtha feedstock by synthesizing a new zeolite with new characterizations.

Keywords: Zeolite; Heavy naphtha; Organic Structural Directing Agent (OSDA); Catalytic reforming process.

DOI: 10.32737/2221-8688-2025-2-187-201

1. Introduction

Naphtha fraction is considered a low octane product that distillates from the topping twoer under atmospheric conditions, it usually ranges between 30-200 °C and constitutes typically 15-30% by weight of the distilled crude oil. This fraction may include some impurities such as nitrogen oxygen, and sulfur compounds. The low-octane naphtha subjected to a reforming process to transform it into a more valuable distillated fraction called reformate which is blended into a pool of gasoline [1]. The reformate fraction typically contains 40–70 wt.% paraffins, 20–50 wt.% naphthenes, and 5-20 wt.% aromatics [2]. Catalytic reforming reaction is one of the main processes for raising the octane number of straight run naphtha fraction, it produces reformate (high aromatic content) with a high octane number by increasing the severity of the reforming reactions. Most reforming units in refineries for gasoline manufacture are designed for high octane number reformate products, resulting in hydrocarbon compounds (C5-C6) reformate yield which typically reaches 80 vol % [3]. This process is regarded as a commercial approach to afford high-octane reformate, and the main target of this manufactured process is to convert paraffinic and naphthenic compounds of naphtha fraction to an aromatic-rich blended product that enhances the gasoline quality and prevents the possibility of pre-ignition in combustion engine [4]. Catalytic internal reforming of naphtha is a key process in industrial petroleum refineries that transforms low-value naphtha fraction (low-octane) into valuable products such as high-octane gasoline [5, 6]. The reforming process includes four main reactions which are dehydrogenation reactions of the normal paraffin to naphthenes then to aromatics, isomerization of paraffin compounds, naphthene iso-form to dehydrocyclization of paraffin to naphthenes, and hydrocracking of naphthenes and paraffin [1, 7, 8]. Mesoporous and microporous zeolite have many promising applications such as improved catalytic stability and activity in various major hydrocarbon conversion processes in the refining and petrochemical industries [9, 10]. Zeolite as a catalyst possesses unique properties, such as strong acidity and hydrothermal stability, which allow it to be employed in many prospective selective reactions. It is well known that the reactivity of zeolites is dependent on the microporous channel structure of Si-Al oxides that are linked to their acidity [11]. Natural zeolite is composed microporous crystalline structure, containing hydrated Al-Si of alkali and alkaline earth cations such as calicium, potassium, sodium, and barium ions. It consists of threedimensional frameworks of silicon (Si⁴⁺) and aluminum (Al³⁺) linked through neighboring oxygen atoms to form a network system of cavities and channels, which facilitate the permeation of several molecules through the zeolitic network [12, 13]. Usually, the cavities are occupied by large ions and water molecules, which determine the shape and size of pores that draw zeolite features such as molecular dimensions. These cations are easily replaced with a wide range of different valency cations, which deploy electrostatic or polarizing molecular forces across the cavities of zeolitic networks. The inserted cation into the cavities by ion exchange process will have different activities of their own; this helps to creat dual function catalysts involving acidity with other activities [14].

It is essential to prepare zeolite with an optimized porous structure in order to provide strength, and locations of acid sites, which can be regarded as Brønsted acid sites [15]. These sites donate protons, which are mainly located inside the pores of zeolite. It is worth mentioning that acid sites are possible reactive centers for acid-catalyzed reactions [16] as shown in Fig 1.

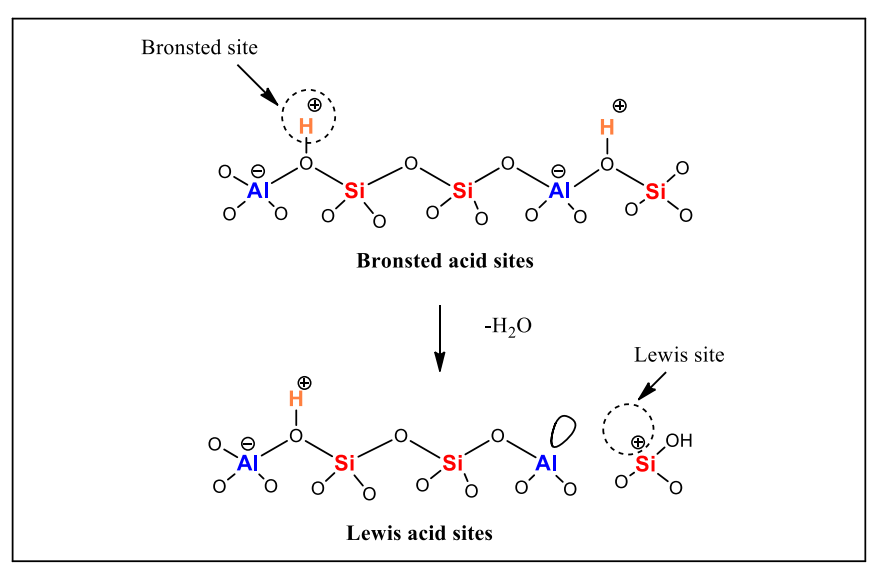


Fig. 1. Formation of Bronsted and Lewis acid sites in zeolite.

Furthermore, absorbed molecules over zeolite pores can be polarized and activated through Lewis acid sites (as acceptors). Moreover, these sites play a vital role towards the catalytic reforming process [17]. The selectivity and activity of zeolite are determined by the Brønsted and Lewis acid sites, which formed by Al substitutions in a zeolite structural framework with the desired porous zeolitic networks [18]. Zeolite synthesis has been investigated and developed using novel methods

of synthesis and the discovery of new zeolitic networks, the application of OSDAs is one of the main approaches having an essential role in the porous zeolitic networks formation as well as the crystallization of the zeolite [19]. Organic compounds such as alkylammonium and alkylamine ions are usually employed as OSDAs, which recognized as one of the main strategies for controlling the Al distribution in the obtained zeolites [18-21]. Several features of OSDAs species dramatically influence the

direction performance of organic structure structural, moieties. and and chemical characteristics of the zeolite framework, utilizing the OSDAs in zeolite synthesis can determine the porous nature of zeolite as well as the hydrothermal stability and rigidity of resulting zeolite [22]. Interestingly, introduction of OSDAs leads to the expansion of the compositional range of crystalline microporous zeolite [23], it also promotes the nucleation and growth of zeolites in the reaction mixture with the non-bonding interaction between the organic moieties and the zeolite frameworks [24]. Furthermore, these synthesis strategies also modify the physicochemical properties resulting of zeolite, architectural changes of the Al distribution over zeolitic networks [11, 23, 25, 26]. Previous studies indicated that a combination of OSDAs such as tetrabutylammonium tetrapropylammonium bromide with aluminosilicate (zeolite) has facilitated the formation of ZSM-5 and ZSM-11, respectively. It was observed that organic specie is one of the major elements having a crucial role in the formation of porous zeolitic frameworks as well as the crystal growth of zeolite. ZSM-5 catalysts exhibited excellent catalytic activity for the conversion methanol to hydrocarbon of compounds [27]. Another study investigated the effect of zeolite Y using a pilot plant unit for the catalytic reforming of naphtha, it was noted the

Research Octane Number (RON) of resulting reformate jumped to 86 with high yield at 520 °C [9]. Recent research showed that the ammonium introduction of tetrapropyl hydroxide as OSDAs with zeolite was found to have the highest crystallinity, suitable morphological structure, effective porous networks. This synthesized zeolite was utilized in a fixed bed reactor at 500 °C under normal pressure to obtain the best catalytic performance of hydrocarbons [28].

The objective of this current study is to investigate a new synthesis pathway of zeolite for catalytic reforming that transforms lowvalue naphtha into a valuable reformate product (gasoline) at a moderate temperature of 300 °C under normal pressure with different residence times. The H-zeolite was prepared using OSDA reagent and subjected to hydrothermal treatment to improve its performance towards catalytic reforming reaction through the modification of the catalyst's acidity and porosity. The synthetic and reformate products evaluated by various techniques to investigate any change in the chemical and physical features of the catalyst and the resulting reformates. Furthermore, results obtained from this current work would further improve our understanding of reaction pathways and find a new approach to enhance the gasoline properties as fuel.

2. Experimental Part

2.1 Materials used.

All the chemicals and reagents with high purity were purchased from Sigma Aldrich and Scientific Fisher. Heavy naphtha feedstock was supplied by the Biji Refinery-Iraq, it is considered a raw material for reforming processes. Characteristics of naphtha were given by the supplier, which are summarized in Table 1. Furthermore, natural zeolitic rock was collected from the north Mosul-Iraq, and then crushed as seeds.

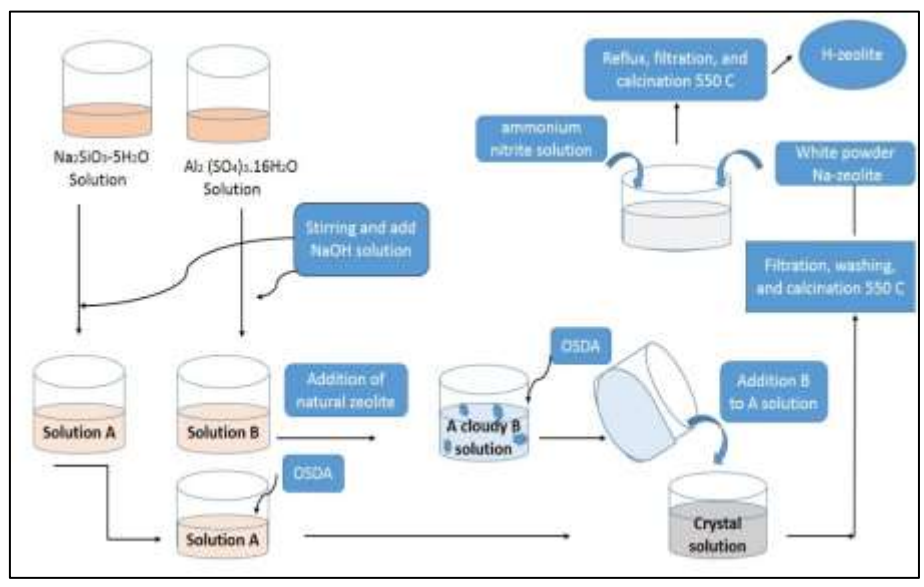
Table 1. Main characteristics of heavy naphtha.

Test	Measurement
Research Octane Number	65
Density at 15 °C	0.7019
Sulfur content (ppm)	0.35
Distillation (I.B.P) (°C)	70
5%	98
50%	132
90%	170
E.P (°C)	200
API	66.1

2.2 Synthesis

The synthetic route of modified zeolite can be described in Scheme 1, which includes

multiple steps to obtain the synthesized zeolite for the naphtha reforming process.



Scheme 1. Schematic diagram for H-zeolite synthesis.

2.2.1. Preparation of Na-Zeolite

The synthesis method of Na-zeolite can be divided into multiple steps, zeolite successfully synthesized according to literature-modified procedure in a previous work by [29, 30] to obtain an amorphous aluminosilicate gel. Zeolite was prepared using hydrothermal synthesis, which includes the formation of hydrated aluminosilicate gel and crystallization. For more details, the silicate and aluminate solutions were synthesized following the procedure by the research group [31]. In separate metasilicate vessels. (sodium aluminum metasilicate-Na₂SiO₃-5H₂O) and sulfate (Al₂ (SO₄)₃.16H₂O) were dissolved in distilled water to produce (25%) silicate and (15%) aluminate solution, respectively. Both resultant mixtures were stirred separately until clear solutions (silicate solution and aluminate) were formed as homogenous solutions at 70 °C. Then the alkaline solution (sodium hydroxide) was added to the silicate and aluminate solution separately until reaching pH= 11 to yield a gelsolution (A) and (B), respectively. The alkaline addition was carried out under vigorous stirring at room temperature for 1 hour. It is worth mentioning that the alkaline attack of the silicate and aluminate-gel results in the desired solutions. After 1h of continuous stirring, clear solutions were formed (solutions A and B). Afterward, natural zeolite (molar composition ratio:3.0 SiO₂: 1.0 Al₂O₃) was poured into solution B. In a typical preparation, natural zeolite was dissolved in aluminate solution (B) to initially form a cloudy mixture (3%) under continuous stirring at ambient temperature for 1 hour. It was observed that the resulting mixture initially transformed into zeolite seeds, which promotes zeolite crystallization on the surface of seeds. In a separate vessel, 4 % of tetramethylammonium bromide (TMA-Br) solution as OSDA reagent was prepared and poured in A and B solution under stirring conditions at 70 °C for 1 hour until completely dissolved to form gel solutions. Eventually, solutions A and B were mixed under stirring for 1 hour at 80 C, resulting in the initial cloudy solution. Then, the hydrothermal crystallization was performed on the resultant mixture at 80 $^{\circ}$ for 72 hours. After the crystallization was achieved, the zeolite solution was cooled down. filtered, and washed with distilled water until the pH value of the filtrate attained to 9, followed by drying in an oven at 80°C for 48 hours. After drying, the product was calcined at 550 C in a furnace for 3 hours in order to decompose OSDA reagent from the zeolite matrix. Na-zeolite product was obtained as a white powder and stored for the next step.

2.2.2. Conversion of Na-Zeolite to H-Zeolite

The resulting Na-zeolite was converted to H-zeolite described in the modified as procedures [31-33]. The synthetic Na-zeolite was treated with ammonium nitrite solution (1 M, 100 mL) and then heated to reflux for 2 hours. The ammonium-zeolite was formed by ion exchange. After refluxing, the resulting solution was cooled down, and the precipitated material was collected via filter paper and then washed many times with distilled water to remove excess ammonium nitrite. Finally, the resulting zeolite was calcined at 550 °C for 3 hours before being cooled to room temperature; this would release (NH₃) and form H-zeolite. The catalyst was obtained as a white powder.

2.2.3. Characterization of catalyst

The X-ray diffraction (XRD) of the natural zeolite and catalyst was performed on an X-ray diffractometer using Ni-filtered Cu K α radiation with a scanning angle (2-Theta- θ) of 10 to 80° with a step size of 10°, this technique was employed to investigate the crystallinity phase of the sample. The XRD pattern of the catalyst was obtained using XRD model (Philips X1 Pert Pro -MPD). The chemical composition of the natural zeolite and its derivative was evaluated using XRF analysis (G.N.R- TX -2000 apparatus). Scanning electron micrographs (SEM) were used to study the morphological features of synthetic zeolite by (Fesem Tescan Mira3) microscope model. Brunauer-Emmett-Teller (BET) technique (The micromeritics, Tri Star II plus, Porosity analyzer) was employed to investigate the sample surface area, and pore size distribution.

2.2.4. Catalytic reforming and H-Zeolite performance

The reforming reactions of naphtha were performed using Teflon-lined autoclaves under atmospheric pressure according to a modified procedure [34]. Essentially, the autoclave consists of a fixed bed carbon steel reactor (23 cm length, 1 cm thickness, and 9.55 cm O.D.)

that equipped with control and heating systems. Each experiment was conducted by charging the reactor with 50 mL naphtha and 2% H-Zeolite as a catalyst then carefully blending. Three catalytic reforming reactions were carried out at 300 C within the residence time ranging from 1 to 3 hours under normal pressure of 1 atm. Naphtha as feedstock was pumped and passed through the catalyst bed, and the reaction took place at a defined temperature. In each experiment at specific conditions, the reforming system was cooled down and the resulting mixture was filtered off using filter paper, and then the filtrate (reformate) was transferred to a glass container for analysis.

2.2.5. Reformate properties

The naphtha feedstock and reformate products have been evaluated to determine the chemical properties and their performance as fuel, different techniques were employed including RON, PIONA-GC-Mass, FTIR, and ¹H NMR. RON is a major feature of gasoline to determine the knock resistance of fuel. RON of samples was measured according to the standard method (ASTM-D2699) [35]. PIONA technique was carried out for the analysis of paraffine, isoparaffine, olefin, naphthene, and aromatic compositions in hydrocarbon samples PIONA -DANI- Master GC-Mass according to ASTM D5134 [36]. FTIR spectroscopy is considered an analytical technique used to determine the functional groups in compounds and compound mixtures using a spectrometer (FTIR- ATR Platinum Bruker). The spectra obtained range from 400–4000 cm⁻¹. The proton $(^{1}H$ magnetic resonance experiments were carried out on all the samples at the normal temperature using a Varian 400 MHz spectrometer. All samples were dissolved in deuterated DMSO, and the chemical shifts were measured relative to tetramethylsilane TMS.

3. Result and discussion

3.1 Characterizations of H-Zeolite

Various techniques were employed to identify the natural raw and synthesized H-zeolites. XRD analysis was utilized to determine the morphological and crystal structures of zeolites. XRD profile of natural zeolitic material

(Figure 2) showed the distinctive sharp peaks which correspond to the crystalline nature of the minerals of which the raw material is composed. According to XRD spectrum, the natural zeolite is mainly composed of montmorillonite clay ((Na, Ca)_{0.33}(Al, Mg)₂(Si₄O₁₀)(OH)₂.nH₂O),

which exhibits the diffraction peaks at $2\theta = 21$, 27, and 68 respectively. Moreover, the other peaks at $2\theta = 12$, 35, 37, 61, and 62 are corresponding to kaolinite component

Al₂(Si₂O₅)(OH)₄. Other mineral groups also exist such as quartz, calcite, and hematite in the raw material as listed in Table 2.

Table 2. Minera	logical and	l chemical	composition of	of natural zeolite

Zeolite constituents	Chemical structures
Montmorillonite	(Na,Ca) _{0.33} (Al,Mg) ₂ (Si ₄ O ₁₀)(OH) ₂ .nH ₂ O
Quartz	SiO ₂
Kaolinite	$Al_2(Si_2O_5)(OH)_4$
Calcite	CaCO ₃
Hematite	Fe ₂ O ₃

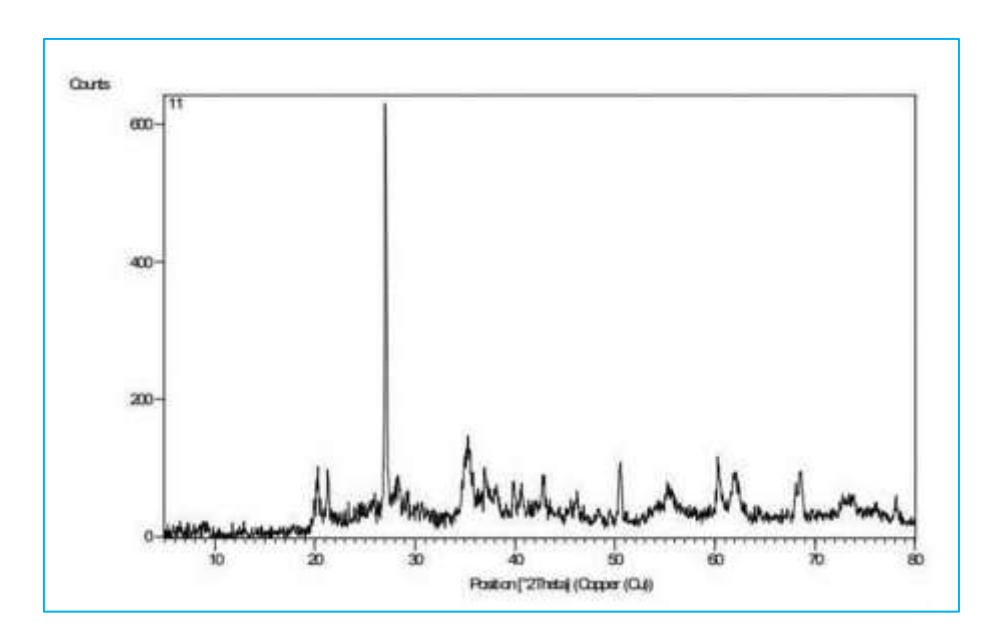


Fig. 2. XRD profile of natural zeolite

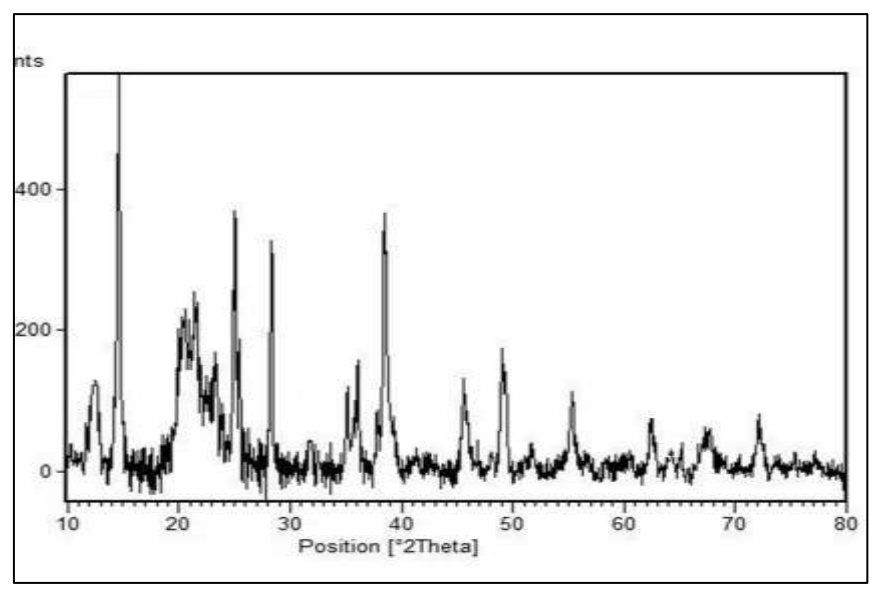


Fig. 3. XRD pattern of modified zeolite using OSDAs.

XRD pattern of H-zeolite exhibited higher crystallinity as illustrated in Fig. 3. The sharp

diffraction peaks of the zeolite appeared at 2θ values that range from 10 to 40° . It is assumed

synthesized H-zeolite has crystalline structures. It is speculated that the utilization of OSDA moieties with zeolite synthesis would increase the crystalline conformations. It can be concluded that **OSDAs** affected the crystallization step by promoting the formation of the regular architecture of frameworks due to the organic molecules interacting with the zeolite surface during the modification process of natural zeolite. Interestingly, the resulting data are consistent with previous studies concerning the influence of OSDAs such as TMA+ on the crystallinity of synthesized zeolite Y [37].

The elemental analysis of natural zeolite and H-zeolite was performed using X-ray fluorescence. This technique was employed to determine of chemical composition of the synthetic zeolite sample. The XRF results exhibited the chemical compositions of raw material and H-zeolite obtained, which are summarized in Table 3.

Table 3. Results of X-ray fluorescence (XRF) analysis of the natural zeolite and synthetic zeolite.

No	Chemical	XRF analysis in	Chemical	XRF analysis in	
	constituents	wt.%	constituents	wt.%	
	of natural zeolite		of modified zeolite		
1	SiO ₂	50.90	SiO_2	64.47	
2	Al_2O_3	17.90	Al_2O_3	22.36	
3			Na ₂ O	8.52	
4	K ₂ O	2.70	K_2O	0.85	
5	Fe ₂ O ₃	5.23	Fe_2O_3	0.73	
6	CaO	12.41	CaO	1.04	
7	MgO	7.10	MgO	0.03	
8	Others	3.70	Others	1.82	
9	SiO ₂ /Al ₂ O ₃ ratio	2.84	SiO ₂ /Al ₂ O ₃ ratio	2.88	

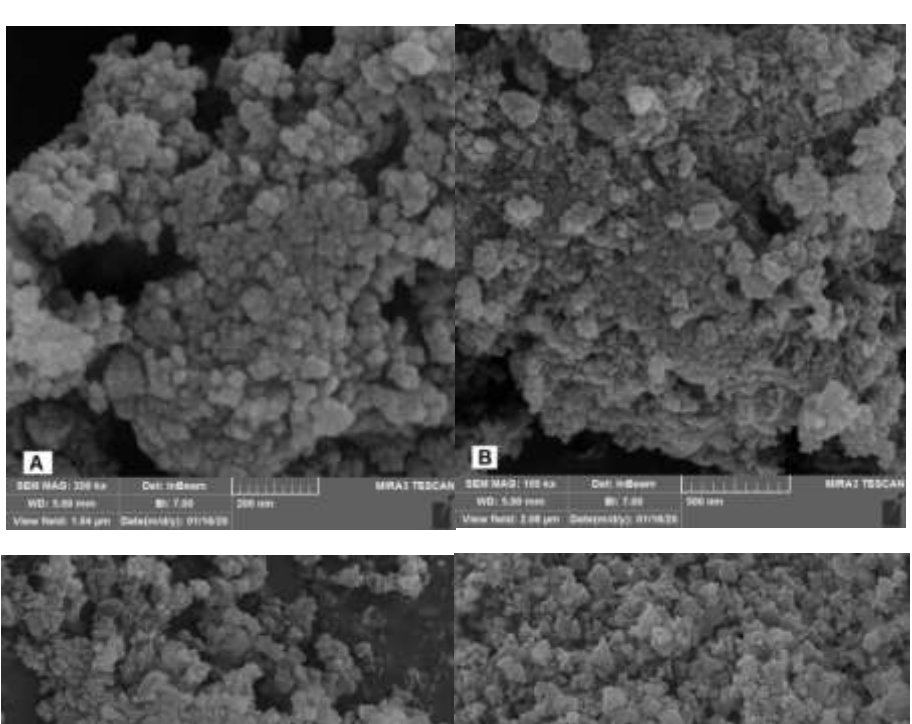
XRF analysis showed that silica is the major constituent of zeolite, containing 50.9 % by weight, followed by alumina (17.9 %). Moreover, raw zeolite tends to have a low percentage of calcium, potassium, magnesium, and ferric oxides, which are a source of various cations. Metal cations (Ca ⁺², Mg⁺², K⁺¹, and F⁺³) balance the negative charge of the zeolitic framework. In addition, these mobile cations impact zeolite's pore and cavity size. In our study, small sizes of cations in natural zeolite would form small pores and channels, resulting in high selectivity of the catalyst toward absorption or reactions.

XRF analysis of modified zeolite revealed that the silica SiO₂ was 64.47% while that of alumina Al₂O₃ was 22.36 %. The ratio SiO₂/Al₂O₃ was 2.88:1. The results showed that the SiO₂/Al₂O₃ ratio of H-zeolite after modification is not different from that of natural zeolite used [38].

The SEM images showed a uniform particle size with a regular spherical shape of the H-zeolite prepared. Micrographs were presented at specific magnifications of 200 Kx, 100 Kx, 50 Kx, and 25 Kx, which exhibited the

morphological characterization of zeolites surface as shown in Fig. 4 A, B, C, and D, respectively. It was observed that granular crystalline microstructure surface and crystal pattern were formed due to the effect of OSDA on the morphological features of synthesized zeolite. The SEM results obtained are in good agreement with previous studies [10, 34, 39].

The BET analysis was performed to determine the pore volume and specific surface area of H-zeolite as tabulated in Table 4. According to the BET analysis, the surface area and the porous volume of H-zeolite are 78.86 m²/g and 0.29246 cm³/g, respectively. These results reflected inter-crystalline voids in the packing of synthesized zeolite. Thus, a large surface can be attributed to the microporous size at 14.4 nm. It can be noted that the surface area of zeolite increased after modification by 13.34 m²/cm³. After the modification of zeolite, the degree of crystallinity increased the specific surface area and the pore volume. On the other hand, the average pore size of the synthesized zeolite decreased to 11 nm when compared to its counterpart (natural zeolite), this could be due to the influence of OSDA moieties, which introduced onto the internal structure and then calcination process. removed from zeolite framework after



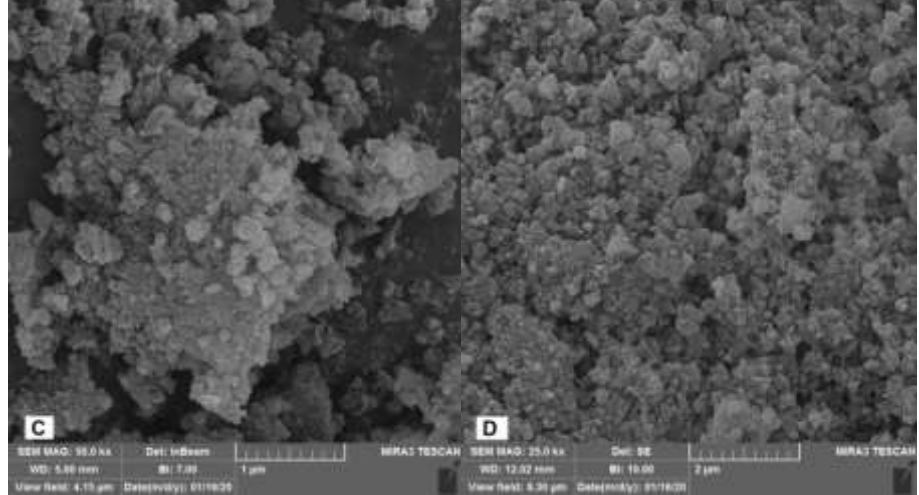


Fig. 4. SEM images of synthesized H-zeolite at different magnifications.

Table 4. BET analysis of natural and modified zeolite.

Sample	Surface area (m ² /g)	Pore volume (cm ³ /g)	Pore Size (nm)	Average particle size (nm)			
	(III /g)	(CIII /g)		Size (IIII)			
Natural zeolite	65.52	0.27	14.60	131.35			
Modified zeolite	78.86	0.29	14.41	120.93			

3.2. Performance of zeolite

The catalytic activity of modified zeolite was evaluated at a defined temperature by different reaction times using straight-run heavy naphtha as the feedstock as shown in Table 5. Naphtha feedstock was pumped and passed through H-zeolite catalyst in the autoclave at 300 C, and then three reactions were carried out at different reaction times separately. In this research, we study the impact of the catalyst structure and porosity on the reformate products

from heavy naphtha using various techniques including PIONA, RON, FTIR, and ¹H NMR. The resulting data of PIONA, which performed on the naphtha and reformate products, are illustrated in Table 5 and Fig. 5. The PIONA analysis shows that the feedstock consists of 41.7% paraffin, 3.4% olefins, 32.1% isoparaffin, 13.6% naphthene, and 9.2% aromatics. From the results obtained, most paraffinic and iso-paraffinic compounds of naphtha were targeted by the synthetic zeolite through a

catalytic reforming process, as the percentage of paraffinic component was reduced initially from 41.7% to 39.2%, while iso-paraffinic compound percentage was risen initially from 32.1% to 35.2%. This can be attributed to the conversion of the paraffin and iso-paraffine in heavy naphtha to aromatic compounds of 12.3% during the first hour of the reaction. The aromatic content in the gasoline reformate increased to 16.4 % when conducting the reforming reaction for two hours. Furthermore,

the last run reaction, which lasted for 3 hours, yielded a gasoline reformate with high RON (85) and high aromatic content of 19.3% The obtained data from Table 5 exhibited that the best catalytic performance was achieved by loading 2% wt of H-zeolite after 3 hours of reaction at 300 °C. This could be due to the selectivity of the catalyst towards cyclization and isomerization reactions over its porous networks [40, 41].

Table 5. PIONA anal	ysis of feedstoc	ck and reformates.
----------------------------	------------------	--------------------

Sample	Reaction	Reaction	RON	Aromatic	Paraffin	Iso-	Olefins	Naphthenics
No.	temperature	time		%	%	paraffins%	%	%
	(°C)	(hour)						
1	-	-	65	9.2	41.7	32.1	3.4	13.6
2	300	1	77	12.3	39.2	35.8	3.2	9.5
3	300	2	81	16.4	35.0	39.7	2.8	6.1
4	300	3	85	19.3	31.1	41.9	2.4	5.3

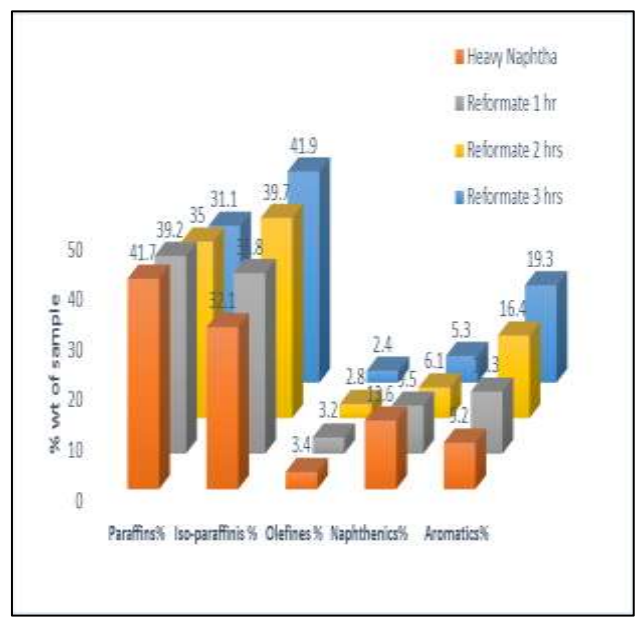


Fig. 5. PIONA analysis of heavy naphtha feedstock and reformate products.

As mentioned above, the ratio Si/Al of the catalyst used was 2.88:1, high Si/Al ratio enhanced the selectivity of zeolite. A recent study by Golubev and his group [42] revealed that the increase of Si/Al ratio in zeolite catalyst led to the increase of selectivity of catalyst toward the middle hydrocarbon distillates. Different post-synthetic modifications of zeolite are employed. one of these modifications is the dealumination from zeolite, which increases Si/Al ratio, it is a widespread approach to reduce the acidity of zeolites, resulting in a

decrease of the unit cell size and the strength of Brønsted acid sites. However, the zeolite activity in cracking and hydrocracking of various hydrocarbon feedstocks dropped with an increase in the Si/Al ratio in the catalyst. this can be probably attributed to a decrease in acid site concentration in the zeolitic network [10]. The synthesized zeolite at Si/Al ratio = 5 was investigated by Nada et.al. [9]. The catalyst showed a high activity toward the reforming reaction of heavy naphtha.

The feedstock reforming over the H-zeolite by thermal treatment exhibited more selectivity towards the cyclization and isomerization reactions to afford more isoparaffinic and aromatic compounds; it could be due to an increase in the acid sites into zeolite frameworks after the modification process.

The catalytic conversion of naphtha was evaluated by RON, this test is one of the most important quality parameters to characterize the naphtha and reformate product. It is employed to evaluate the performance of the internal

combustion engine. RON of naphtha feedstock improved dramatically after performing the reforming reactions for an hour in the presence of H-zeolite, reaching 77, and then RON value jumped to 81 after 2 hours, the RON value increased to 85 after conducting the reforming reaction for 3 hours as a result of catalyst activation. It was observed that increasing reaction time enhanced the catalytic stability and conversion rate of naphtha, which led to a higher yield of aromatic content and consequently higher RON.

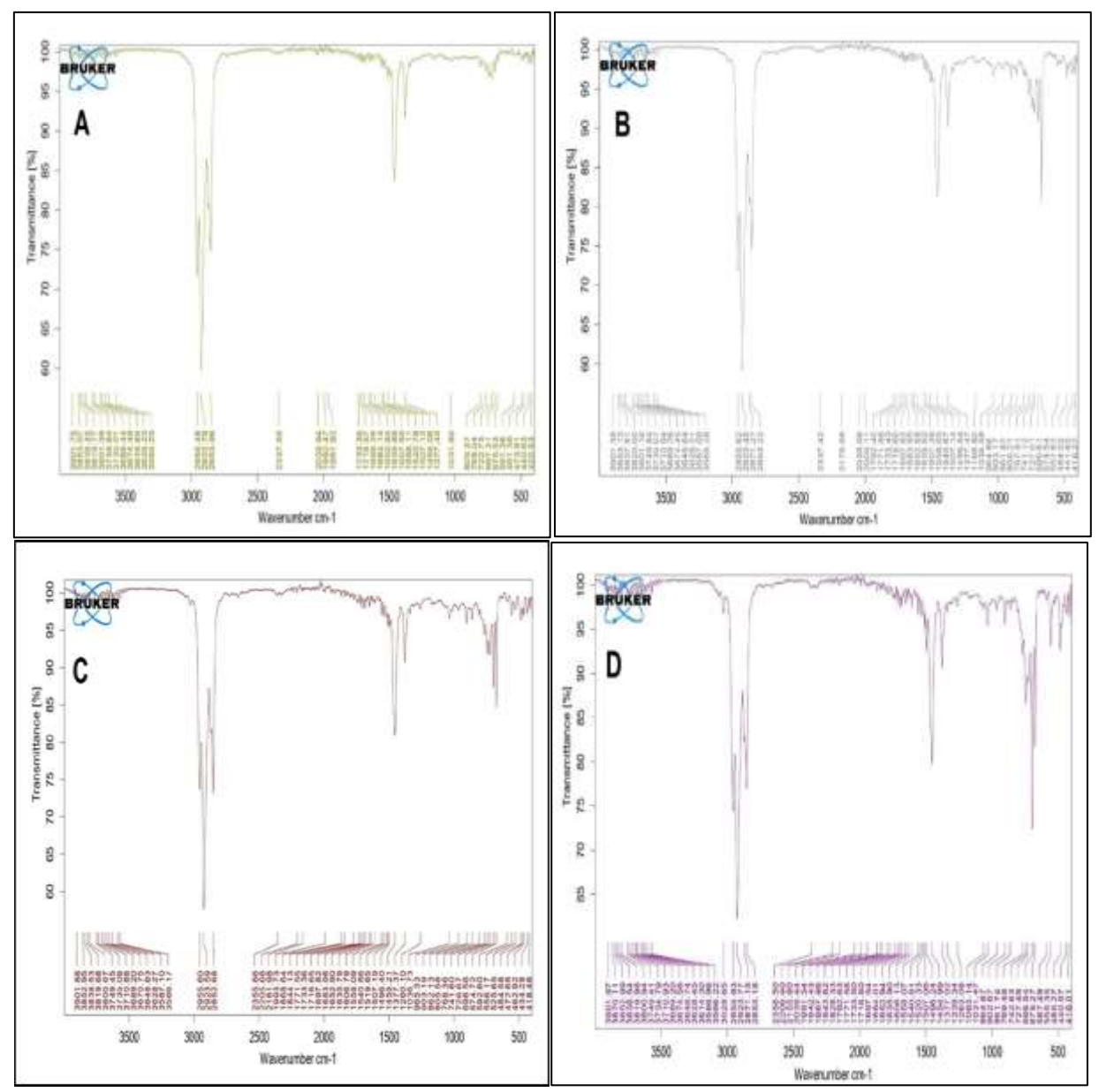


Fig. 6. FTIR spectrum of naphtha (A), reformate for 1 hr (B), reformate for 2 hrs (C), and reformate for 3 hrs (D).

FTIR spectrum (Fig. 6 A) of the naphtha signals between 2853-2955 cm⁻¹ refers to the

presence of -CH-aliphatic stretch. Other sharp peaks appear at 1377 and 1485 cm⁻¹, which

indicate the -CH for the methyl group. The low-intensity peaks in the range between 675 and 722 cm⁻¹ indicate the presence of aromatic compounds such as substituted benzene. Fig. 6 B, C, and D revealed that distinctive peaks of gasoline reformates are observed in the fingerprint region between 650 and 750 cm⁻¹, this could be due to the high content of aromatic compounds in the samples [43].

In order to further interpret the chemical features of heavy naphtha and its derivatives, ¹H NMR spectrum of samples was conducted to determine the position of proton in the untreated and treated samples. (Fig. 7 A, B, C, and D)

revealed that ¹H NMR spectra contain a large number of overlapping signals belonging to different hydrocarbon types. It can be noticed that intensities of integrated proton peaks are proportional to the proton number in each functional group in the hydrocarbon complexity of each sample. The numerical values of the integral protons allow evaluating their percentage without prior calibration. The ¹H-NMR spectra of feedstock, as shown in Fig. 7A, exhibited distinctive peaks at 0-3 chemical shifts, which indicates the presence of aliphatic protons in heavy naphtha compounds.

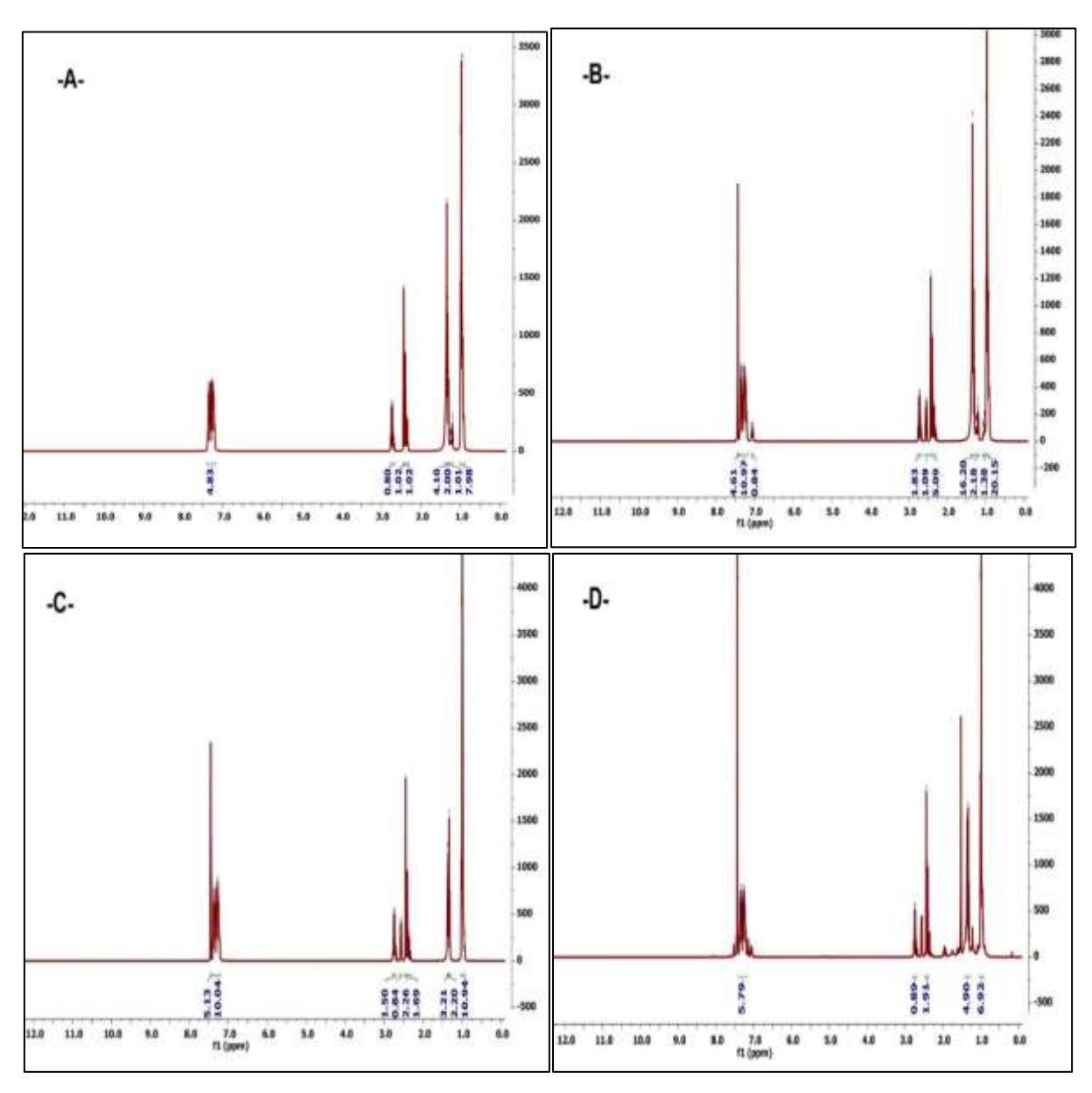


Fig. 7. ¹H-NMR spectrum of heavy naphtha (A), treated naphtha for 1 hr (B), treated naphtha for 2 hrs (C), treated naphtha for 3 hrs (D).

The other multi-peaks appear between 7.20-7.35 chemical shifts that indicate the presence of mono and polyaromatic protons in naphtha feedstock. By comparing the results for naphtha and gasoline reformates. It is found that the aromatic content, at the aromatic region (7-7.5 ppm) for gasoline reformate samples, is substantially enhanced via signal intensities

when compared with the heavy naphtha sample. This observation is due to the more aromatic compounds produced during the reforming process for gasoline reformates products at different conditions. It is worth mentioning that the ¹H-NMR chemical shift of naphtha studied is in excellent agreement with previous studies [43, 44].

4. Conclusion

In this current study, H-zeolite was successfully synthesized from natural zeolite using OSDA (tetramethylammonium bromide) reagent through thermal treatment. ODSA was designed for the zeolites expected to be most promising for the catalytic reforming process. Furthermore, OSDA showed strong interactions with the zeolite framework, which resulted in more ordered structures and porous. This study discusses the influence of the modification technique on zeolite activity and selectivity in improving aromatic content during naphtha

Conflicts of Interest

The authors declare no conflict of interest.

Acknowledgments

We greatly thank Mosul University for funding support.

References

1. Yusuf A.Z., Aderemi B.O., Patel R., Mujtaba I.M. Study of industrial naphtha catalytic reforming reactions via modelling and simulation. *Processes*, 2019, **Vol. 7(4)**, p. 192. https://doi.org/10.3390/pr7040192.

- 2. George A., Di B., Modern Electroplating. 2011, John Wiley and Sons, Hoboken, 729 p. 10.1002/9780470602638.ch12.
- 3. Parkash S. Petroleum fuels manufacturing handbook: including specialty products and sustainable manufacturing techniques. 2010, 1st ed., McGraw-Hill Education.
- 4. Lee S. Encyclopedia of chemical processing. 2006, 1st Edition, Taylor & Francis US. https://doi.org/10.1201/NOE0824755638.
- 5. Lapinski M.P., Metro S., Pujadó P. R., Moser M. Catalytic reforming in petroleum processing. Handbook of Petroleum Processing, 2015, 2. https://doi.org/10.1007/978-3-319-05545-9_1-1.

reforming reactions. The synthesized catalyst revealed activity towards the catalytic reforming reaction of heavy naphtha as feedstock. The results of the catalytic tests showed that the zeolite had excellent catalytic activity toward the reforming of heavy naphtha. Zeolite with different residence times exhibited a vital role in the enhancement of RON of the resulting product via catalytic reforming. This is probably due to enhancing the yield of aromatics in each reformate sample by the reforming process.

- S., Ahmed **Optimizing** Saleh A.A., Bioethanol Production for High Octane Bioethanol-Gasoline Blended Fuel through Fermentation. Journal of the Turkish Chemical Society Section A: Chemistry, 2023. Vol. 10(2), 475-486. p. https://doi.org/10.18596/jotcsa.1250955
- 7. Ahmedzeki N.S., Al-Tabbakh Antwan M.B., Yilmaz S. Heavy naphtha upgrading by catalytic reforming over novel bi-functional zeolite catalyst. Reaction kinetics, mechanisms and catalysis, 2018, Vol. 125, 1127-1138. p. https://doi.org/10.1007/s11144-018-1432-y.
- 8. Karimov A. Optimal design of the oxidative dehydrogenation of methylcyclohexane into methylcyclohexadiene on a modified zeolite catalyst. *Chemical Problems*, 2022, **Vol. 20(1)**, p. 48-58. https://doi.org/10.32737/2221-8688-2022-1-48-58

- 9. Ahmedzeki N.S., Al-Tabbakh B.A. Catalytic reforming of Iraqi naphtha over Pt-Ti/HY zeolite catalyst. *Iraqi Journal of Chemical and Petroleum Engineering*, 2016, **Vol. 17(3)**, p. 45-56. https://doi.org/10.31699/IJCPE.2016.3.4.
- Al-Shafei E.N., Albahar M.Z., Aljishi M.F., Akah A., Aljishi A.N., Alasseel A. Catalytic conversion of heavy naphtha to reformate over the phosphorus-ZSM-5 catalyst at a lower reforming temperature. *RSC advances*, 2022, Vol. 12(39), p. 25465-25477. https://doi.org/10.1039/D2RA04092A.
- 11. Palčić A., Valtchev V. Analysis and control of acid sites in zeolites. *Applied Catalysis A: General*, 2020, **Vol. 606**, p. 117795. https://doi.org/10.1016/j.apcata.2020.117795.
- Rodríguez-Castro L.M., Urbiztondo-Castro M., Pina-Iritia M.P. Influence of boehmite intermediate layer as covalent linker on synthesis of LTA zeolite coatings. *Revista Facultad de Ingeniería Universidad de Antioquia*, 2021, Vol. 101, p. 64-73. https://doi.org/10.17533/udea.redin.2020069

13.Montalvo

- S., Guerrero L., Borja R., Sánchez E., Milán Zh., Cortés I., de la Rubia M. A. Application of natural zeolites in anaerobic digestion processes: A review. *Applied Clay Science*, 2012, **Vol. 58**, p. 125-133. https://doi.org/10.1016/j.clay.2012.01.013
- 14. Ugal J.R., Hassan K.H., Ali I.H. Preparation of type 4A zeolite from Iraqi kaolin: Characterization and properties measurements. *Journal of the Association of Arab Universities for Basic and Applied Sciences*, 2010, **Vol. 9(1)**, p. 2-5. https://doi.org/10.1016/j.jaubas.2010.12.00 2.
- 15. Vorontsov A.V., Smirniotis P.G., Kumar U. A DFT Study on Single Brønsted Acid Sites in Zeolite Beta and Their Interaction with Probe Molecules. *Catalysts*, 2023, **Vol. 13(5)**, p. 833. https://doi.org/10.3390/catal13050833.
- Chizallet C., Bouchy Ch., Larmier K., Pirngruber G. Molecular Views on Mechanisms of Brønsted Acid-Catalyzed Reactions in Zeolites. *Chemical Reviews*,

- 2023, **Vol. 123(9)**, p. 6107-6196. https://doi.org/10.1021/acs.chemrev.2c0089
- Tsaplin D.E., Ostroumova V.A., Kulikov L.A., Zolotukhina A.V., Sadovnikov A.A., Kryuchkov M.D., Egazaryants S.V., Maksimov A.L., Wang K., Luo Zh., Naranov E.R. Synthesis and Investigation of Zeolite TiO2/Al-ZSM-12 Structure and Properties. *Catalysts*, 2023, Vol. 13(2), p. 216. https://doi.org/10.3390/catal13020216.
- 18. Bae J., Dusselier M. Synthesis strategies to control the Al distribution in zeolites: thermodynamic and kinetic aspects. *Chemical Communications*, 2023, **Vol. 59(7)**, p. 852-867. https://doi.org/10.1039/D2CC05370E.
- 19. Pour A.Z., Sebakhy K.O. A Review on the Effects of Organic Structure-Directing Agents on the Hydrothermal Synthesis and Physicochemical Properties of Zeolites. *Chemistry*, 2022, **Vol. 4(2)**, p. 431-446. https://doi.org/10.3390/chemistry4020032.
- 20. Meng L., Mezari B., Goesten M.G., Wannapakdee W., Pestman R., Gao L., Wiesfeld J., Hensen E.J.M. Direct synthesis of hierarchical ZSM-5 zeolite using cetyltrimethylammonium as structure directing agent for methanol-to-hydrocarbons conversion. *Catalysis Science & Technology*, 2017, **Vol. 7(19)**, p. 4520-4533.
 - https://doi.org/10.1039/C7CY01603D.
- 21. Al-AzzawiA.G., Iraqi A., Aziz Sh.B., Zhang Y ., Murad A.R., Hadi J.M., Lidzey D.G. Synthesis, **Optical** and Electrochemical **Properties** of Naphthothiadiazole-Based Donor-Acceptor Polymers and Their Photovoltaic Applications. Int. J. Electrochem. Sci, 2021, Vol. 16(21125), https://doi.org/10.20964/2021.12.32
- 22. Gómez-Hortigüela L., Camblor M.A. Introduction to the zeolite structure-directing phenomenon by organic species: general aspects. Insights into the chemistry of organic structure-directing agents in the synthesis of zeolitic materials, 2018, p. 1-41. https://doi.org/10.1007/430_2017_8.

- 23. Simancas R., Chokkalingam A., Elangovan Sh.P., Liu Z., Sano T., Iyoki Okubo K., Wakihara T., T. Recent progress in the improvement of hydrothermal stability of zeolites. Chemical science, 2021, Vol. 12(22), p. 7677-7695. https://doi.org/10.1039/D1SC01179K.
- 24. Daeyaert F., Deem M.W. Design of organic structure directing agents to guide the synthesis of zeolites for the separation of ethylene–ethane mixtures. *RSC advances*, 2020, **Vol. 10(34)**, p. 20313-20321. https://doi.org/10.1039/D0RA02896G.
- 25. Sadoon A.M. Theoretical Investigation of the Structures and Energetics of (MX)-Ethanol Complexes in the Gas Phase. *Journal of the Turkish Chemical Society Section A: Chemistry*, 2023, **Vol. 10(1)**, p. 47-54. https://doi.org/10.18596/jotcsa.1146250.
- 26. Al-Azzawi A.G., Ghazal R.Y. Evaluation of Rheological and Thermal Behavior of Polymer Modified Asphalt. *Egyptian Journal of Chemistry*, 2022, **Vol. 65(11)**, p. 1-10. https://doi.org/10.21608/ejchem.2022.1212 28.5446.
- 27. Zenonos C., Sankar G., García-Martínez J., Aliev A., Beale A.M. Direct hydrothermal conversion of high-silica faujausite and zeolite β to Zsm-5 and its catalytic performance. *Catalysis letters*, 2003, **Vol. 86**, p. 279-283. https://doi.org/10.1023/A:1022688623543.
- Sanhoob M.A., Khan A., Ummer A.C. ZSM-5 Catalysts for MTO: Effect and optimization of the tetrapropylammonium hydroxide concentration on synthesis and performance. ACS omega, 2022, Vol. 7(25), p. 21654-21663. https://doi.org/10.1021/acsomega.2c01539.
- Abid R., Delahay G., Tounsi H. Preparation of LTA, HS and FAU/EMT intergrowth zeolites from aluminum scraps and industrial metasilicate. *Journal of Material Cycles and Waste Management*, 2019, Vol. 21, p. 1188-1196. https://doi.org/10.1007/s10163-019-00873-x.
- 30. Tounsi H., Mseddi S., Djemel S. Preparation and characterization of Na-LTA zeolite from Tunisian sand and aluminum scrap.

- Physics Procedia, 2009, Vol. 2(3), p. 1065-1074.
- https://doi.org/10.1016/j.phpro.2009.11.064
- 31. Liu Z., Shi Ch., Wu D., He Sh., Ren B. A simple method of preparation of high silica zeolite y and its performance in the catalytic cracking of cumene. *Journal of Nanotechnology*, 2016, **Vol. 2016**, https://doi.org/10.1155/2016/1486107.
- 32. Petrov A.W., Ferri D., Krumeich F., Nachtegaal M., van Bokhoven J.A., Kröcher O. Stable complete methane oxidation over palladium based zeolite catalysts. *Nature communications*, 2018, Vol. 9(1), p. 2545. https://doi.org/10.1038/s41467-018-04748-x.
- 33. Sugiarti S., Septian D.D., Maigita H., Khoerunnisa N.A., Hasanah S., Wukirsari T., Hanif N., Apriliyanto Y.B. Investigation of H-zeolite and metal-impregnated zeolites as transformation catalysts of glucose to hydroxymethylfurfural. in AIP Conference Proceedings, 2020, AIP Publishing. https://doi.org/10.1063/5.0001789.
- 34. Nabgan W., Nabgan B., Tuan Abdullah T.A., Ali M.W. Development of zeolites for zeoforming reaction of naphtha. *Malaysian Journal of Catalysis*, 2021, **Vol. 5(1)**. https://doi.org/10.11113/mjcat.v5n1.155
- 35. Testing A.S.F. Standard Test Method for Research Octane Number of Spark-ignition Engine Fuel. 2018, ASTM.
- 36. Silva A.P., Bahú J.O., Soccol R., Rodríguez-Urrego L., Fajardo-Moreno W.S., Moya H., León-Pulido J., Cárdenas Concha V.O. Naphtha characterization (PIONA, density, distillation curve and sulfur content): An origin comparison. *Energies*, 2023, **Vol. 16(8)**, p. 3568. https://doi.org/10.3390/en16083568
- 37. Goretsky A.V., Beck L.W., Zones S.I., Davis M.E. Influence of the hydrophobic character of structure-directing agents for the synthesis of pure-silica zeolites. *Microporous and Mesoporous Materials*, 1999, **Vol. 28(3)**, p. 387-393. https://doi.org/10.1016/S1387-1811(98)00307-2.
- 38. Krisnandi Y.K., Saragi I.R., Sihombing R., Ekananda R., Sari I.P., Griffith B.E., Hanna J.V. Synthesis and characterization of

- crystalline NaY-Zeolite from Belitung Kaolin as catalyst for n-Hexadecane cracking. *Crystals*, 2019, **Vol. 9(8)**, p. 404. https://doi.org/10.3390/cryst9080404.
- 39. Oyebanji J., Okekunle P., Fayomi O. Synthesis and characterization of zeolite-Y using Ficus exasperata leaf: A preliminary study. *Case Studies in Chemical and Environmental Engineering*, 2020, **Vol. 2**, p. 100063.
 - https://doi.org/10.1016/j.cscee.2020.100063.
- 40. Khudyakov I.V., Levin P.P., Efremkin A.F. Cage Effect under Photolysis in Polymer Matrices. *Coatings*, 2019, **Vol. 9(2)**, p. 111. https://doi.org/10.3390/coatings9020111
- 41. Che Y., Yuan M., Qiao Y., Liu Q., Zhang J., Tian Y. Fundamental study of hierarchical millisecond gas-phase catalytic cracking process for enhancing the production of light olefins from vacuum residue. *Fuel*, 2019, **Vol. 237**, p. 1-9. https://doi.org/10.1016/j.fuel.2018.09.088.
- 42. Golubev I., Dik P.P., Kazakov M.O., Pereyma V.Yu., Klimov O.V.,

- Smirnova M.Yu., Prosvirin I.P., Gerasimov E.Yu., Kondrashev D.O., Golovachev V.A., Vedernikov O.S., Kleimenov A.V., Noskov A.S. The effect of Si/Al ratio of zeolite Y in NiW catalyst for second stage hydrocracking. *Catalysis today*, 2021, **Vol. 378**, p. 65-74. https://doi.org/10.1016/j.cattod.2021.01.014
- 43. Rajasekar Maruthamuthu A., S., Muthukumar N.. Mohanan S., Subramanian P., Palaniswamy N. Bacterial degradation of naphtha and its influence on corrosion. Corrosion Science, 2005. Vol. 47(1), 257-271. p. https://doi.org/10.1016/j.corsci.2004.05.016
- 44. Won S.H., Lim S.J., Nates S., Alwahaibi A.K., Dryer F.L., Farid F., Hase M. Combustion characteristics of crude oils for gas turbine applications by DCN measurements and NMR spectroscopy. *Proceedings of the Combustion Institute*, 2021, **Vol. 38(4)**, p. 5463-5473.

https://doi.org/10.1016/j.proci.2020.06.184.